

Electrical Properties and Scaling Behavior of AgO Thin Films

¹Rawia AbdElgani Elobaid, ²Nafisa Bader Eldeen, ³Aldesogi Omer Hamed, ⁴Ali Sulaiman Mohamed, ⁵Bashir Elhaj Ahmed & ⁶Sawsan Ahmed Elhourri Ahmed

^{1,2} Sudan University of Science & Technology - College of Science
Department of Physics - Khartoum - Sudan

^{3,4} Omdurman Islamic University - Faculty of Science and Technology
Department of Physics - Omdurman – Sudan

⁵Al-Neenlen University – Faculty of Science and Technology
Department of Physics - Khartoum- Sudan

⁶University of Bahri - College of Applied & Industrial Sciences
Department of Physics - Khartoum- Sudan

Abstract

The AgO sample, prepared by chemical reaction technique. The compound shows significant frequency dispersion in its dielectric properties. The scaling behavior of dielectric loss and imaginary electric modulus suggest that the relaxation describe same mechanism at various temperatures. Impedance data presented in the Nyquist plot (Z_{00} versus Z_0) are used to identify an equivalent circuit and to know the bulk and interface contributions. The complex impedance analysis of AgO exhibits the appearance of both the grain and the grain-boundary contribution. The frequency dependent conductivity spectra follow the universal power law. The magnitude of the activation energy indicates that the carrier transport is due to the hopping conduction.

Keywords: Spray pyrolysis, dielectric, imaginary electric, complex impedance, thin films, AgO

Introduction

Most of the I-III-VI₂ compounds are direct gap semiconductors and they crystallize with the chalcopyrite structure [1, 2]. They have attracted a lot of attention due to their potential applications in opto-electronic and photovoltaic devices. Although the information on Ag chalcopyrite compounds are scarce compared with Cu compounds, there is many studies about Ag compounds are found [3, 4]. Among the various thin film deposition techniques, spray pyrolysis is one of the principle methods used to produce a large area and uniform coating at

simple and low cost [5]. It is well known that the optical properties of thin films are highly sensitive to the preparation conditions and treatment conditions [6].

The interaction of laser beams with solid surfaces produce a variety of surface morphology changes, many of which show ripple structure with periods comparable to optical wavelength [7, 8]. Energy-beam shaping can be used to prevent heterogeneous nucleation and promote growth of long individual grains. Argon laser offers the potential for good control over the recrystallization process because of the ability to produce a narrow molten zone and to shape the beam with a variety of optical techniques. In this paper, deposition of AgO thin films by chemical spray pyrolysis and the effect of thermal annealing and laser radiation optical properties of thin films are studied [9].

Material & Method

0.5 g of silver nitrate (AgNO_3) solid was dissolved in 10mL of distilled water in a 100mL beaker. Then, triethanolamine TEA solution was added drop wise with constant stirring until the initially formed precipitate was dissolved (brownish solution becomes colorless). More distilled water was added to make a total volume of 80 mL. The pH of the bath was 8.0. Glass slides that have been preleased by degreasing in concentrated H_2SO_4 , washed with water and detergent and rinsed with distilled water were vertically placed into the beaker and the bath was brought to and kept at 50°C on a hot plate. After various periods of time 90 min, the coated four slides were removed from the bath, thoroughly rinsed with distilled water, and air-dried using electrical hand drier. The films were annealed at ($100, 150$ and 200°C) for better adhesion and homogeneity on the substrates.

For the electrical measurement the sintered disc was polished to make both their faces flat and parallel and electroded by highpurity ultrafine silver paste. To overcome the effect of moisture, on electric properties. Capacitance (C), impedance (Z), phase angle (ω) and conductance (G), of the sample was measured in the frequency range $100 \text{ Hz} - 1 \text{ MHz}$ at various temperatures using a computercontrolled LCR-meter . The complex electric modulus

$M^* = (1/\epsilon^*)$, the complex impedance $Z^* (=1/\omega C_0 \epsilon^*)$ and the ac electrical conductivity $s (= \omega \epsilon_0 \epsilon_{00})$ were obtained from the temperature dependence of the real (ϵ_0) and imaginary (ϵ_{00}) components of the complex dielectric constant $\epsilon^* = (\epsilon_0 - \epsilon_{00})$, $\omega = (2\pi\nu)$ [10,11,12].

Results and Discussion

Dielectric relaxation study the angular frequency $\omega = (2\pi\nu)$, ν is the frequency of ac field) dependence of real (ϵ_0) and imaginary parts (ϵ_{00}) of the complex dielectric permittivity (ϵ^*) of Ag O as a function of temperature is shown in Fig (1). A relaxation is observed in the entire temperature range as a gradual decrease in $\epsilon_0(\omega)$ and a broad peak in $\epsilon_0(\omega)$. The variation of ϵ_0 with frequency explains frequency relaxation phenomena of the material which are associated with a frequency dependent orientation polarization. If the frequency of the applied ac is much lower than the inverse of relaxation time (τ) of the dipoles (i.e. $\omega \ll 1/\tau$), the situation is essentially as for dc i.e. electric dipoles follow the field and we have $\epsilon_0 \sim \epsilon_s$ (ϵ_s = low frequency value of ϵ_0 or value of dielectric constant at quasi-static fields). At very high frequency ($\omega \gg 1/\tau$), dipoles responsible for the polarization can no longer be able to follow the oscillations of the electric field and $\epsilon_0 \sim \epsilon_1$ (ϵ_1 = high frequency value of ϵ_0). The field reversal and the dipole reorientation becomes out-of-phase, giving rise to an energy dissipation within the sample at a particular frequency. Such an effect is called dielectric relaxation and may be evidenced by a drop in ϵ_0 and a maximum in the imaginary part of the permittivity (ϵ_{00}) at the relaxation frequency Fig (2). The peak position of ϵ_{00} , centered at the dispersion region of ϵ_0 , shifts to higher frequency with increasing temperature Fig (2). The increase in angular frequency corresponding to ϵ_{00} maximum with temperature indicates an increase in charge carriers in the sample by thermal activation. It should be noted that the sharp increase in ϵ_{00} at low frequencies is due to the presence of dc conductivity. At low frequencies the ac conductivity is similar to dc conductivity (δ_{dc}). So δ_{dc} has an observable influence on the loss component of the dielectric response when it is relatively large. With increasing frequency, the influence of δ_{dc} would be ignorable. This kind of dependence of loss components on frequency is typically associated with losses by conduction. It seems clear that the width of the loss peaks Fig (2) cannot be accounted for in terms of a mono dispersive relaxation process but points towards the possibility of distribution of relaxation times. One of the most convenient ways to determine the poly dispersive nature of the dielectric relaxation is through Cole–Cole model where the complex dielectric constant (ϵ^*) is described by the empirical relation [13]:

$$\epsilon^* = \epsilon_0 - i\epsilon_0 = \epsilon_\infty + \frac{\epsilon_s - \epsilon_\infty}{1 + (i\omega\tau)^{1-\alpha}} \quad (1)$$

Whereas is the low frequency value and ϵ_1 is the high frequency value of ϵ_0 , α is a measure of distribution of relaxation times, $\omega = (2\pi\nu)$ is the angular frequency of applied ac field and $\tau = \omega^{-1}$ is the most probable relaxation time, $\tau = \sqrt{-1}$. We have fitted the experimental data using equation (1). The fitted data are shown in Fig (2), giving the values of (α) to be between 0.10 and 0.17 for the temperature range from 100 to 200°C. A good agreement between the directly measured values of (ϵ_{00}) and those calculated using equation (1) suggests that the relaxation process differs from the monodispersive Debye process (for which $\alpha = 0$). As an alternate approach, the polydispersive nature of dielectric relaxation of AgO can also be confirmed by a representative complex Argand plane plots between (ϵ_{00}) and (ϵ_0) for $(T = 100, 150 \text{ and } 200)^\circ\text{C}$ as shown in Fig(3). For a pure monodispersive Debye process, one expects semicircular plots with a centre located on the (ϵ_0) axis whereas, for polydispersive relaxation process ($\alpha \neq 0$), these Argand plane plots are close to circular arcs with end points on the axis of reals and a centre below this axis. The parameter α , can be determined from the angle subtended by the radius of Cole–Cole circle with the (ϵ_0) axis and is found to be 0.28 radian at 30 8C. The scaling behaviour of ϵ_{00} is shown in Fig (3) for AgO. We have scaled each (ϵ_{00}) by $(\epsilon_{00})_m$ ($(\epsilon_{00})_m$ is the peak value of loss ϵ_{00}) and each frequency by ν_m (ν_m is the frequency corresponding to $(\epsilon_{00})_m$ i.e. the frequency at which (ϵ_{00}) was found to be maximum). The overlapping of curves at various temperatures into a single master curve indicates that the relaxation describes the same mechanism at various temperatures in AgO. For the measurement of the characteristic relaxation time (τ_m) , we can choose the inverse of frequency of the peak position of (ϵ_{00}) versus $\log \nu$ plots in Fig (3) i.e. $\tau_m = \omega_m^{-1}$. The temperature dependence of the characteristic relaxation time is shown in the inset of Fig (3), which satisfy the Arrhenius law: $\omega_m \tau_m \exp(E_a / k_B T) = 1$. From the numerical fitting analysis, we have obtained the value of the activation energy $E_{\epsilon_{00}} = 0.35 \text{ eV}$ for the material ($E_{\epsilon_{00}}$ represents activation energy of ϵ_{00} obtained from the peak position of ϵ_{00} versus $\log \nu$ plots). Such a value of activation energy indicates that the conduction mechanism in AgO may be due to the polaron hopping based on the electron carriers. In the hopping process, the electron distorts its surrounding by moving its neighboring atoms in the B-sites of the perovskite system.

The electrical properties of the material were determined by impedance spectroscopy. Experimental complex impedance data may well be approximated by the impedance of an equivalent circuit consists of resistors, capacitors and possibly various distributed circuit elements. These equivalent circuit can be physically interpreted and assign them to appropriate process. The display of impedance data in complex plane plot appears in the form of a succession of semicircles attributed to relaxation phenomena with different time constants due to

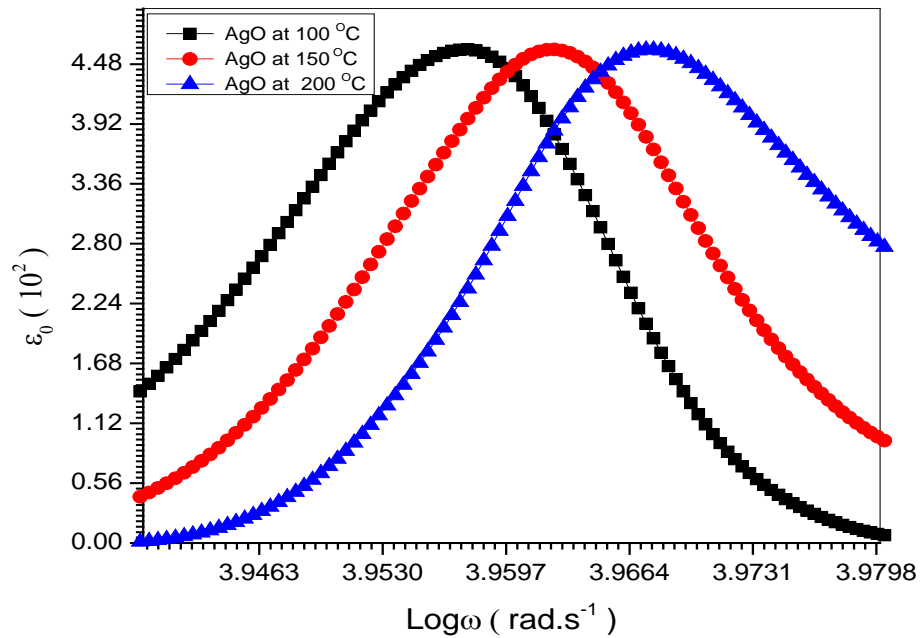
the contribution of grain, grain-boundary and interface/electrode polarization in the polycrystalline materials. Hence the contribution to the overall electrical properties by various components in the material are separated out easily. Cole–Cole representation is more convenient to distinguish between the bulk and grain boundary effects [14]. The complex impedance plane plot (Z^{**} Vs. Z^*) where real Z^* represents the resistive part and imaginary Z^{**} represents the capacitive part is generally used. Fig. (4) presents a typical complex impedance plane plot of AgO ceramic and the corresponding equivalent circuit (inset of Fig.(4) at 100, 150 and 200 °C. The two well resolved semicircular arcs on this complex plane plot are attributed to the grain and grain-boundary effect. The values of grain and grain-boundary resistances and capacitances can be obtained by an equivalent circuit of two parallel resistance-capacitance (RC) elements connected in series. The equivalent electrical equations for grain and grain boundary are

$$Z^* = R_s + \frac{R_g}{1+(\omega R_g C_g)^2} + \frac{R_{gb}}{1+(\omega R_{gb} C_{gb})^2} \quad (2)$$

And

$$Z^{**} = R_g \left[\frac{\omega R_g C_g}{1+(\omega R_g C_g)^2} \right] + R_{gb} \left[\frac{\omega R_{gb} C_{gb}}{1+(\omega R_{gb} C_{gb})^2} \right] \quad (3)$$

Where, R_s is the series resistance, Z^* and Z^{**} are the real and imaginary parts of complex impedance (Z^*), C_g and C_{gb} are the grain and grain-boundary capacitances and R_g and R_{gb} are the grain and grain-boundary resistances. We have fitted our experimental data with equations (2) and (3) as shown by solid lines in Fig.(4). The fitted parameters for R_g are 6.83, 6.75 and 4.52 MV at temperatures 100, 150 and 200 °C respectively and the corresponding grain capacitance (C_g) values are 7.81×10^{-11} , 8.50×10^{-11} , 8.62×10^{-11} F. Similarly, the grain-boundary resistance (R_{gb}) values at 100, 150 and 200 °C are 12.68, 12.50 and 11.64 MV respectively. And the corresponding grain-boundary capacitance (C_{gb}) values are 9.45×10^{-11} , 9.58×10^{-11} , and 10^{-11} F.



Fig

Fig.(1):Angular frequency dependence of (ϵ_0)of AgO at various Temperatures at (100, 150, 200 °C).

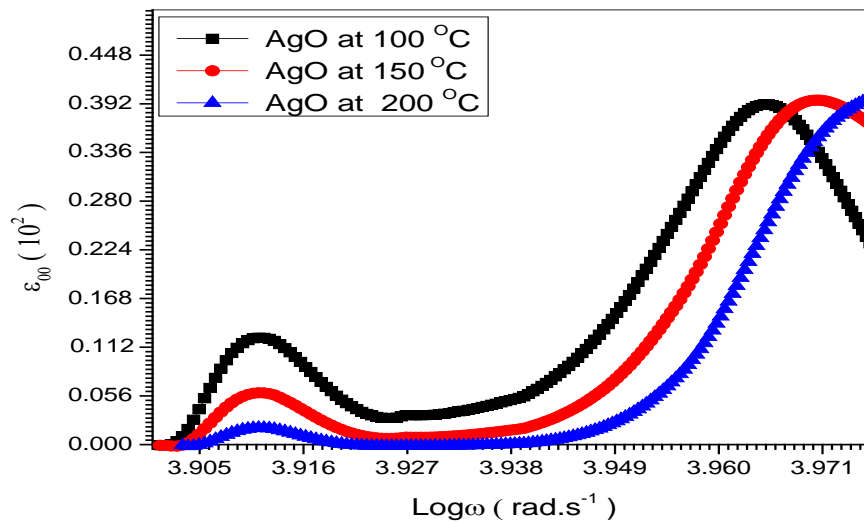


Fig. (2): Angular frequency dependence of (ϵ_{00}) of AgO at various Temperatures at(100, 150, 200 °C)

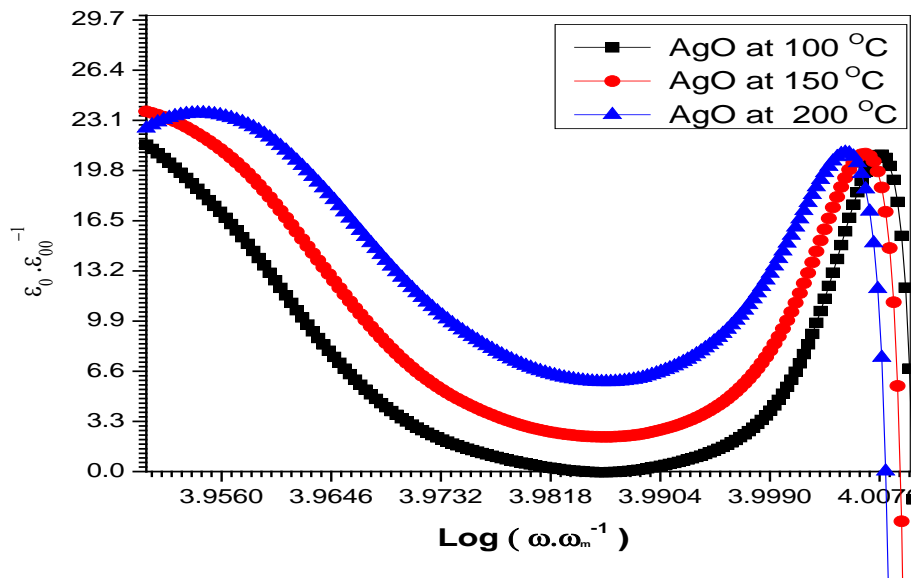


Fig.(3):Scaling behavior of (ϵ_{00})at various temperatures for Ag Oat 100, 150, 200 °C.

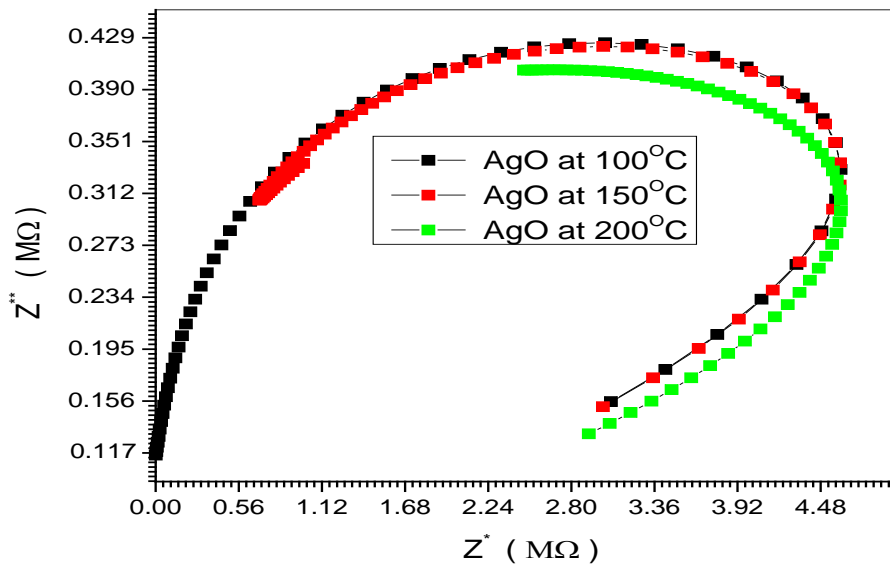


Fig.(4):Complex plane plot of impedance for Ag O at 100, 150, 200 °C

References

- [1] S.F.Shaukat ,S.A.Khan and R.Farooq:Turk.J.Phys.31(2007) pp.(265-269)
- [2]B. H. Patel and S.S. Patel: Cryst. Res. Technol. 41 (2006) No.2, pp. 117-122.
- [3] D. N. Okoli, A. J. Ekpunobi and C. E. Okeke : Academic open internet journal . (2006) Vol.18, Issue.1311-4360.
- [4] M. L. Albor-Aguilera, J. J. Cayente-Romero, J. M. Peza-Tapia, L. R. De León-Gutierrez and M. Ortega-López : Thin Solid Films , (2005).Vol. 490 , Issues. 2, pp. 168-172.
- [5] H.V. Campe: Thin Solid Films, (1984) Vol. 111, Issues.1, pp. 17-35.
- [6] A. Jagomägi , JüriKrustok , JaanRaudoja, MaarjaGrossderg , Ilona Oja , MalleKrunks and Mati Danilson : Thin Sold Films , (2004) Vol. 480-481, pp. 246-249.
- [7] B.Thangaraju and P.Kaliannan: Cryst.Res.Technol. (2000)Vol. 35, No.1, pp.(77-75).
- [8] J. Nayayan, W.L.Brown and R.A.Lemons: Materials Research Society,(1983) Vol.13, p.191 and 523.
- [9] M.T. Anderson, K.B. Greenwood, G.A. Taylor, K.R. Poepelmeier, Prog. Solid StateChem. 22 (1993) 197.
- [10] Y. Tomioka, T. Ocuda, Y. Okimoto, R. Kumai, K.I. Kobayasi, Phys. Rev. B 61 (2000)422.
- [11] N. Rama, J.B. Phillip, M. Opel, V. Sankaranarayanan, R. Cross, M.S. RamachandraRao, J. Phys. D: Appl. Phys. 40 (2003) 1430.
- [12] M.C. Castro, J. Paschoal, F. synder, M. Lufaso, J. Appl. Phys. 104 (2008) 104114.
- [13] (a) K.S. Cole, R.H. Cole, J. Chem. Phys. 9 (1941) 341;(b) K.S. Cole, R.H. Cole, J. Chem. Phys. 10 (1942) 98.
- [14] (a) J.T.S. Irvine, D.C. Sinclair, A.R. West, Adv. Mater. 2 (1990) 132;(b) J.R.M. Donald, Impedance Spectroscopy, John Wiley, New York, 2005.